A collection of Benchmark examples for model reduction of linear time invariant dynamical systems [1]

Younès Chahlaoui and Paul Van Dooren[2]

February 2002

[1]This document presents research results of the European Community BRITE-EURAM III Thematic Networks Programme NICONET (contract number BRRT-CT97-5040) and is distributed by the Working Group on Software WGS. *WGS secretariat*: Mrs. Ida Tassens, ESAT - Katholieke Universiteit Leuven, Kasteelpark Arenberg 10, 3001-Leuven-Heverlee, BELGIUM. This report is available by anonymous ftp from `wgs.esat.kuleuven.ac.be/pub/WGS/REPORTS/SLWN2002-2.ps.Z`
[2]Université Catholique de Louvain, CESAME, B-1348 Louvain-la-Neuve, Belgium

Abstract

In order to test the numerical methods for model reduction we present here a benchmark collection, which contain some useful 'real world' examples reflecting current problems in applications.
All simulations were obtained via **Matlab** and some **slicot** programs of Niconet (see *http://www.win.tue.nl/niconet/niconet.html*).

Contents

1 Introduction

We consider the stable linear time-invariant (LTI) system,

$$\left\{ \begin{array}{rcll} E\delta x(t) & = & Ax(t) + Bu(t), & t > 0, \quad x(0) = x^0, \\ y(t) & = & Cx(t) + Du(t), & t \geq 0 \end{array} \right. \tag{1}$$

and the associated transfer function matrix (TFM),

$$G(\lambda) = C(\lambda E - A)^{-1}B + D \tag{2}$$

with $E, A \in \mathbb{R}^{N\times N}$, $B \in \mathbb{R}^{N\times m}$, $C \in \mathbb{R}^{p\times N}$, and $D \in \mathbb{R}^{p\times m}$. The number of state variables N is said to be the order of the system. If $t \in \mathbb{R}$ and $\delta x(t) = \dot{x}(t)$, the system is a continuous-time system and λ is the frequency variable s, while (1) describes a discrete-time system if $t \in \mathbb{Z}$ and $\delta x(t) = x(t+1)$ is the forward shift operator and λ is in this case z.

The aim is to find a reduced order LTI model,

$$\left\{ \begin{array}{rcll} E_n\delta x_n(t) & = & A_n x_n(t) + B_n u_n(t), & t > 0, \quad x_n(0) = x_n^0, \\ y_n(t) & = & C_n x_n(t) + D_n u_n(t), & t \geq 0 \end{array} \right. \tag{3}$$

of order n, $n \ll N$, such that the TFM $G_n(\lambda) = C_n(\lambda E_n - A_n)^{-1}B_n + D_n$ approximates the first one in a particular sense.

A large class of model reduction methods rely on the construction of matrices : $T_l \in \mathbb{R}^{n\times N}$ and $T_r \in \mathbb{R}^{N\times n}$ such that the reduced model is defined as

$$E_n = T_l E T_r,\ A_n = T_l A T_r,\ B_n = T_l B,\ C_n = C T_r \text{ and } D_n = D.$$

We assume that the generalized spectrum of (A, E), denoted by $\Lambda(A, E)$, is contained in the stable region of the complex plane.

There is no general technique for model reduction that can be considered as optimal in an overall sense since the reliability, performance and adequacy of the reduced system strongly depends on the system characteristics. Model reduction methods usually differ in the error measure they attempt to minimize.

The model reduction methods that we are interested in are strongly related to the controllability Gramian $\mathcal{G}_c$ and the observability Gramian $E^T\mathcal{G}_oE$ of the system $(E^{-1}A, E^{-1}B, C)$ (under the assumption that E is invertible).
For continuous-time systems the Gramians are given by the solutions of two "coupled" (as they share the same coefficient matrix A) Lyapunov equations :

$$A\mathcal{G}_cE^T + E\mathcal{G}_cA^T + BB^T = 0, \quad A^T\mathcal{G}_oE + E^T\mathcal{G}_oA + C^TC = 0$$

while in the discrete-time case, the Gramians satisfy the Stein equations (or discrete Lyapunov equations) :

$$A\mathcal{G}_cA^T - E\mathcal{G}_cE^T + BB^T = 0, \quad A^T\mathcal{G}_oA - E^T\mathcal{G}_oE + C^TC = 0$$

The Hankel Singular Values (HSV) of the systems are given by the square-roots of the eigenvalues of $\mathcal{G}_c E^T \mathcal{G}_o E$, i.e.,

$$\Lambda(\mathcal{G}_c E^T \mathcal{G}_o E) = \{\sigma_1^2, \ldots, \sigma_N^2\}, \quad \sigma_1 \geq \sigma_2 \geq \ldots \geq \sigma_N \geq 0.$$

As the pair (A, E) is assumed to be stable, $\mathcal{G}_c$ and $\mathcal{G}_o$ are positive semi-definite.

Every data file contains the default matrices A, B, C, D and E for descriptor systems. If D, C or E are not given, it means that $D = 0$, $C = B^T$ and $E = I$.
There is also a vector of the Hankel singular values hsv, a frequency vector ω and the corresponding frequency response mag. When $\mathcal{G}_c$ and $\mathcal{G}_o$ are positive definite the data files contain two matrices S and R which are the Cholesky factors of the matrices $\mathcal{G}_c, \mathcal{G}_o$, i.e. $\mathcal{G}_c = S^T S$, $\mathcal{G}_o = R^T R$, rather than the Gramians themselves.
If there are several Gramians corresponding to SISO subsystems, they are denoted with a subscript as well as the corresponding Cholesky factors (e.g. $\mathcal{G}_{c_1}$, S_1, $\ldots$).

Dense models

Data file	N	m	p	Elements
eady.mat	598	1	1	A, B, C, R, S, mag, w
tline.mat	256	2	2	A, B, C, E, $\mathcal{G}_c$ $\mathcal{G}_o$, mag, w

Sparse models

Data file	N	m	p	Elements
CDplayer.mat	120	2	2	A, B, C, R, $R1$, $R2$, S, $S1$, $S2$, hsv, mag, w
peec.mat	480	1	1	A, B, C, E, mag, w
fom.mat	1006	1	1	A, B, C, R, S, hsv, mag, w
random.mat	200	1	1	A, B, C, R, S, hsv, mag, w
pde.mat	84	1	1	A, B, C, R, S, hsv, mag, w
heat-cont.mat	200	1	1	A, B, C, R, S, hsv, mag, w
heat-disc.mat	200	1	1	A, B, C, E, R, S, hsv, mag, w
Orr-Som.mat	200	1	1	A, R, S, hsv, mag, w
MNA_1.mat	578	9	9	A, B, E
MNA_2.mat	9223	18	18	A, B, E
MNA_3.mat	4863	22	22	A, B, E
MNA_4.mat	980	4	4	A, B, E
MNA_5.mat	10913	9	9	A, B, E

Second order models

A second order model is a system of the type:

$$M\ddot{x}(t) + C_d\dot{x}(t) + Kx(t) = B_d u(t)$$

Under the assumption that M is invertible, this system leads to a linear system with the matrices [3]:

$$A = \begin{bmatrix} 0 & I \\ -M^{-1}K & -M^{-1}C_d \end{bmatrix}, \quad B = \begin{bmatrix} 0 \\ M^{-1}B_d \end{bmatrix}$$

C can be taken as B^T or something else.

Data file	N	m	p	Elements
iss.mat	270	3	3	A, B, C, R, $R1$, $R2$, $R3$, S, $S1$, $S2$, $S3$, hsv, mag, w
build.mat	48	1	1	A, B, C, R, S, hsv, mag, w
beam.mat	348	1	1	A, B, C, R, S, hsv, mag, w

2 Benchmarks examples

2.1 Eady example

This is a model of the atmospheric storm track (for example the region in the midlatitude Pacific). The mean flow is taken to be in a periodic channel in the zonal x-direction, $0 < x < 12\pi$, the channel is taken to be bounded with walls in the meridional y-direction located at $y = \pm\frac{\pi}{2}$ and at the ground, $z = 0$, and the tropopause, $z = 1$. The mean velocity is varying only with height and it is $U(z) = 0.2 + z$. Zonal and meridional lengths are nondimensionalized by $L = 1000km$, vertical scales by $H = 10km$, velocity by $U_0 = 30m/s$ and time is nondimensionalized advectively, i.e. $T = \frac{L}{U_0}$, so that a time unit is about $9h$.

In order to simulate the lack of coherence of the cyclone waves around the Earth's atmosphere, an observed characteristic of the Earth's atmosphere, we introduce linear damping at the storm track's entry and exit region. The perturbation variable is the perturbation geopotential height (i.e. the height at which surfaces of constant pressure are located).

The perturbation equations for single harmonic perturbations in the meridional (y) direction of the form $\phi(x, z, t)e^{ily}$ are :

$$\frac{\partial \phi}{\partial t} = \nabla^{-2}\Big[- z\nabla^2 D\phi - r(x)\nabla^2\phi\Big],$$

where ∇^2 is the Laplacian $\frac{\partial^2}{\partial x^2} + \frac{\partial^2}{\partial z^2} - l^2$ and $D = \frac{\partial}{\partial x}$. The linear damping rate $r(x)$ is taken to be $r(x) = h(2 - \tanh[(x - \frac{\pi}{4})/\delta] + \tanh[(x - \frac{7\pi}{2})/\delta])$ ($h = 2.5, \delta = 1.5$).

The boundary conditions are expressing the conservation of potential temperature (entropy) along the solid surfaces at the ground and tropopause:

$$\frac{\partial^2\phi}{\partial t\partial z} = -zD\frac{\partial \phi}{\partial z} + D\phi - r(x)\frac{\partial\phi}{\partial z} \quad \text{at} \quad z = 0,$$

$$\frac{\partial^2\phi}{\partial t\partial z} = -zD\frac{\partial \phi}{\partial z} + D\phi - r(x)\frac{\partial\phi}{\partial z} \quad \text{at} \quad z = 1.$$

Note that these equations are the same for perturbation evolution in a Couette flow with free boundaries.

We write the dynamical system in generalized velocity variables $\psi = (-\nabla^2)^{\frac{1}{2}}\phi$ so that the dynamical system is governed by the dynamical operator:

$$A = (-\nabla^2)^{\frac{1}{2}}\nabla^{-2}\Big(- zD\nabla^2 + r(x)\nabla^2\Big)(-\nabla^2)^{\frac{-1}{2}}.$$

where the boundary equations have rendered the operators invertible. We consider the case $l = 1$. Now the state are governed by the equation:

$$\frac{d\psi}{dt} = A\psi$$

We can define two correlation matrix $\mathcal{G}_c = \int_0^\infty e^{At} e^{A^T t} dt$ and $\mathcal{G}_o = \int_0^\infty e^{A^T t} e^{At} dt$ solution of Lyapunov equations:

$$A\mathcal{G}_c + \mathcal{G}_c A^T + I = 0 \quad , \quad A^T \mathcal{G}_o + \mathcal{G}_o A + I = 0$$

These matrices are the equivalent of the controllability and observability Gramians.

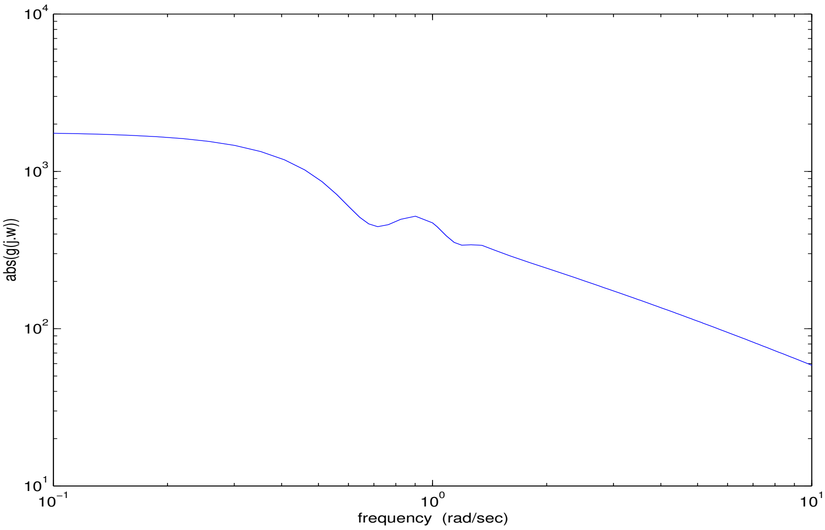

Figure 1: Frequency response.

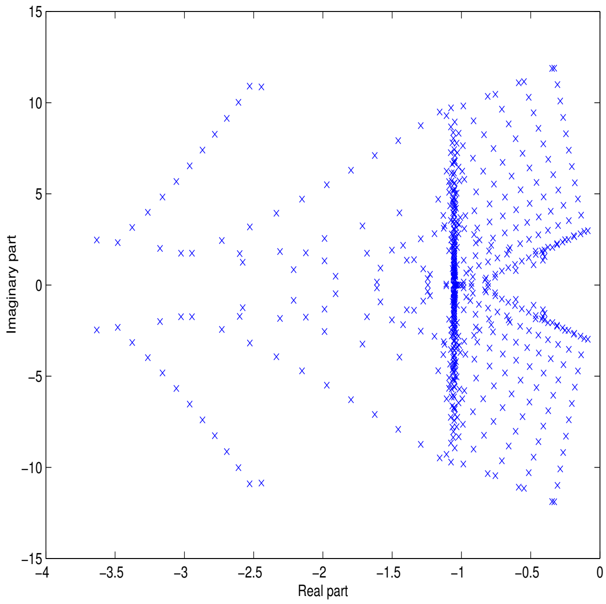

Figure 2: eigenvalues of A

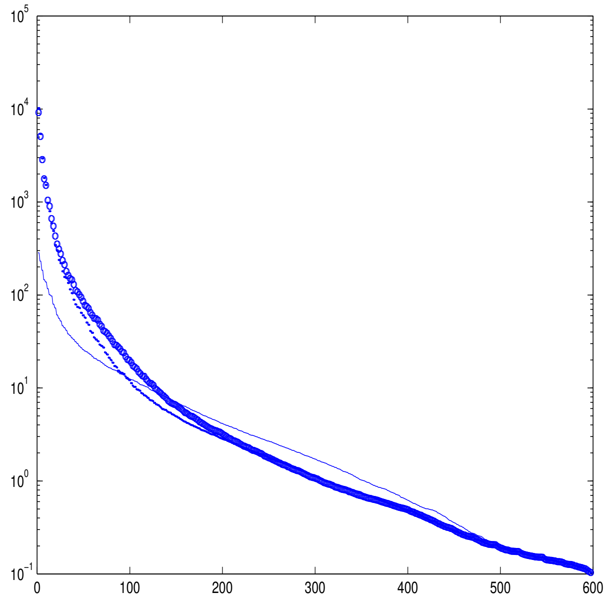

Figure 3: .. svd($\mathcal{G}_c$), o svd($\mathcal{G}_o$), ___ hsv

2.2 Transmission line model

A transmission line is a circuit model modeling the impedence of interconnect structures accounting for both the charge accumulation on the surface of conductors and the current traveling along conductors [8], [9].

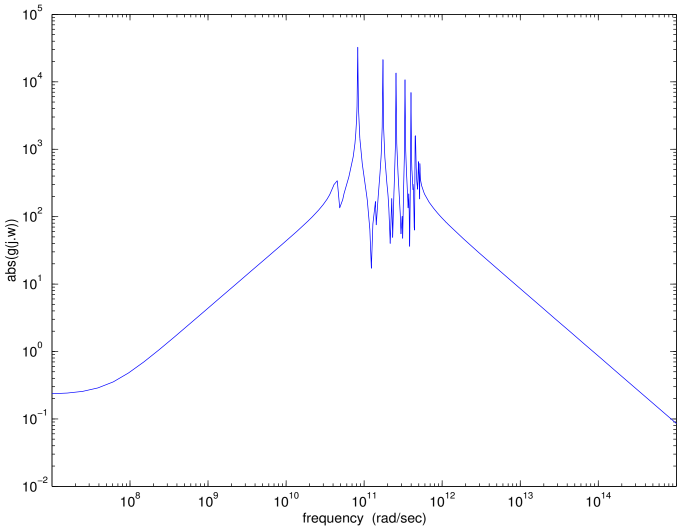

Figure 4: frequency response
1^{st} input / 1^{st} output $\equiv$ 2^{st} input / 2^{st} output.

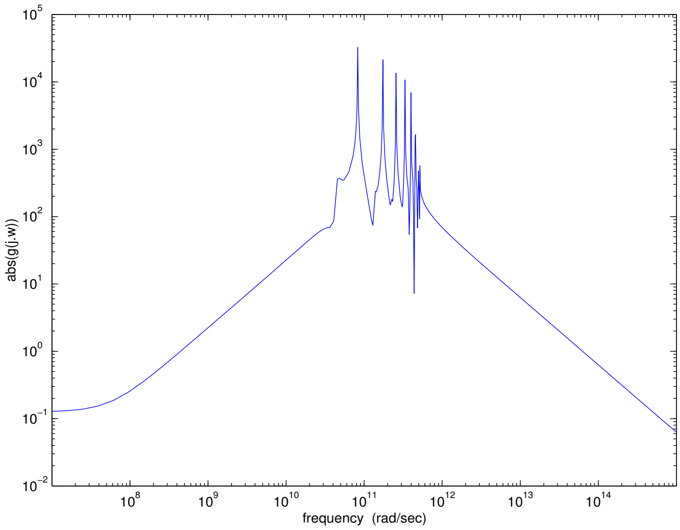

Figure 5: frequency response
1^{st} input / 2^{st} output $\equiv$ 2^{st} input / 1^{st} output.

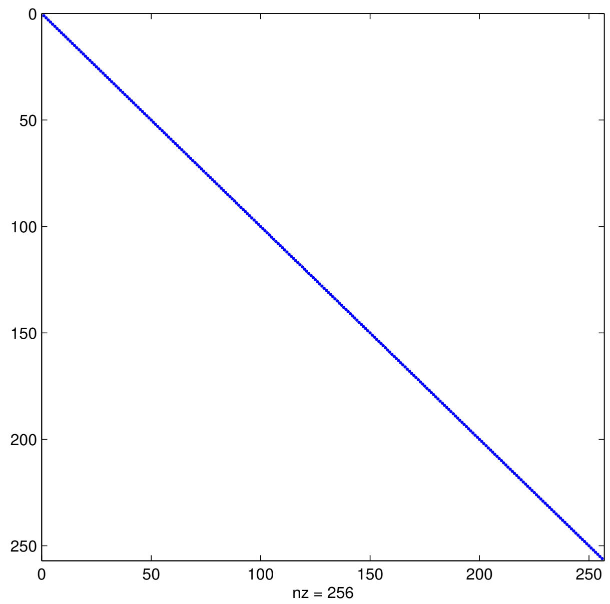

Figure 6: sparsity of A.

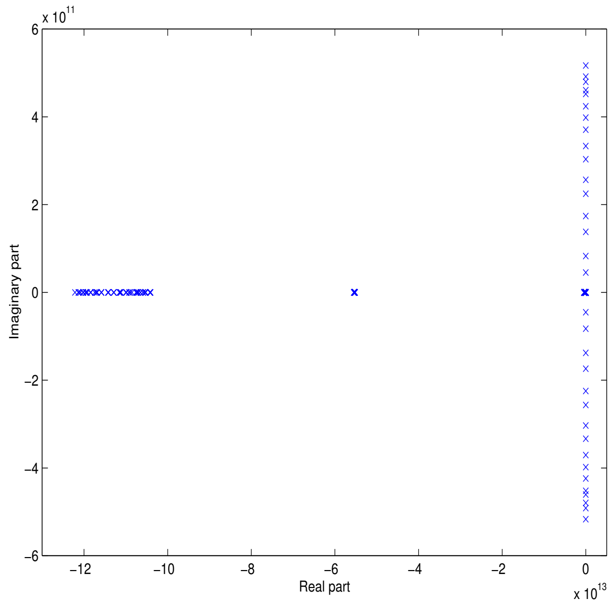

Figure 7: generalized eigenvalues of (A, E).

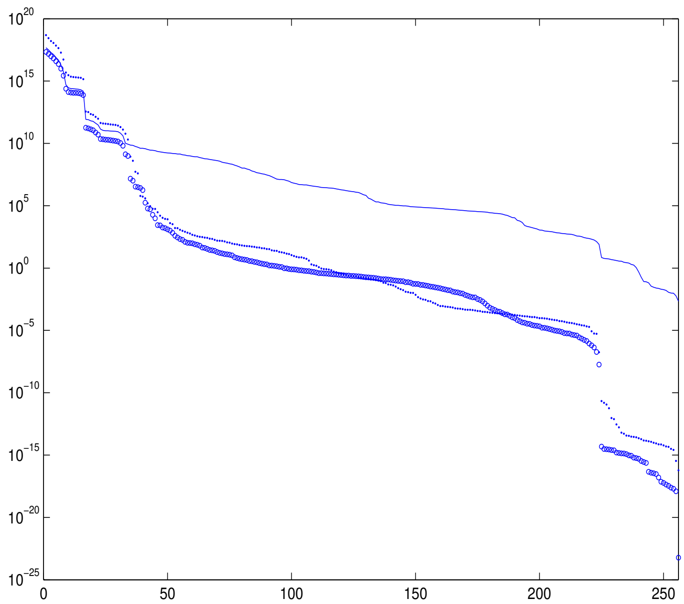

Figure 8: .. svd($\mathcal{G}_c$), o svd($\mathcal{G}_o$), ___ hsv.

2.3 CD player

The control task is to achieve track following, which basically amounts to pointing the laser spot to the track of pits on the CD that is rotating. The mechanism treated here, consists of a swing arm on which a lens is mounted by means of two horizontal leaf springs. The rotation of the arm in the horizontal plane enables reading of the spiral-shaped disc-tracks, and the suspended lens is used to focus the spot on the disc. Due to the fact that the disc is not perfectly flat, and due to irregularities in the spiral of pits on the disc, the challenge is to find a low-cost controller that can make the servo-system faster and less sensitive to external shocks [4] and [13].The model contains 60 vibration modes.

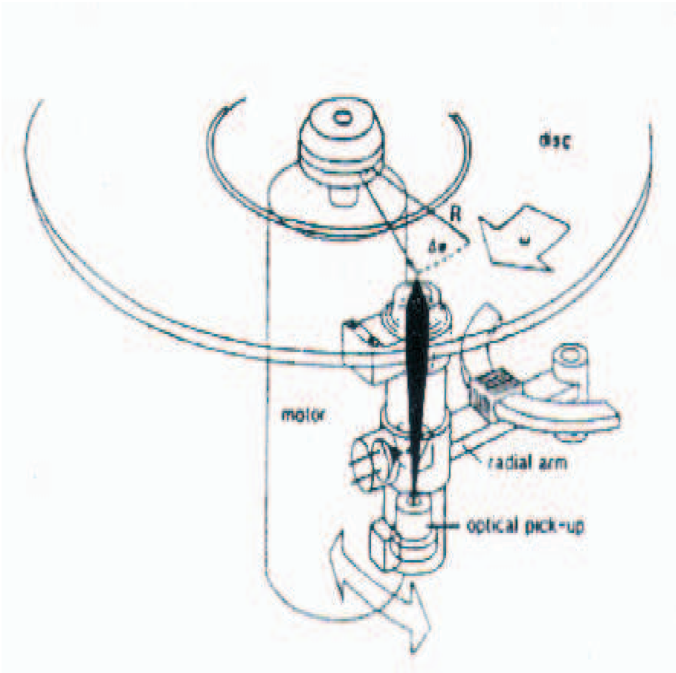

Figure 9: Schematic view of a rotating arm Compact Disc mechanism.

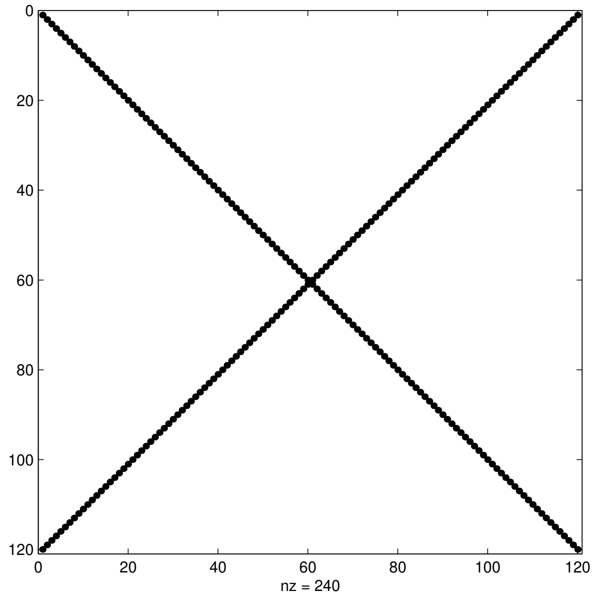

Figure 10: Sparsity of A.

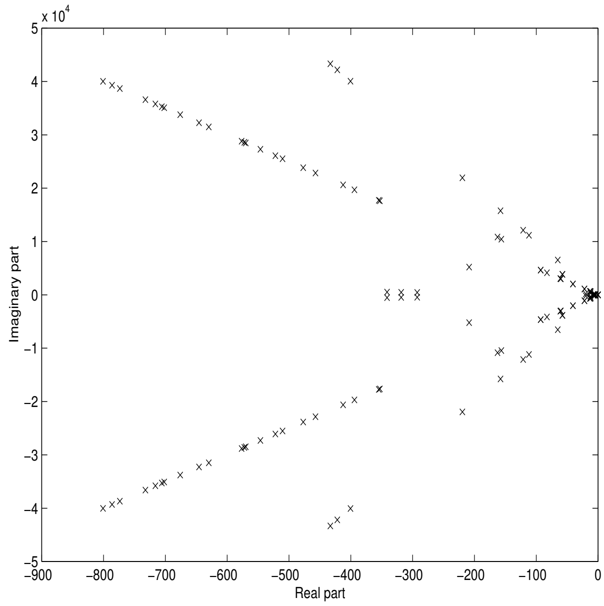

Figure 11: Eigenvalues of A (stable but lightly damped).

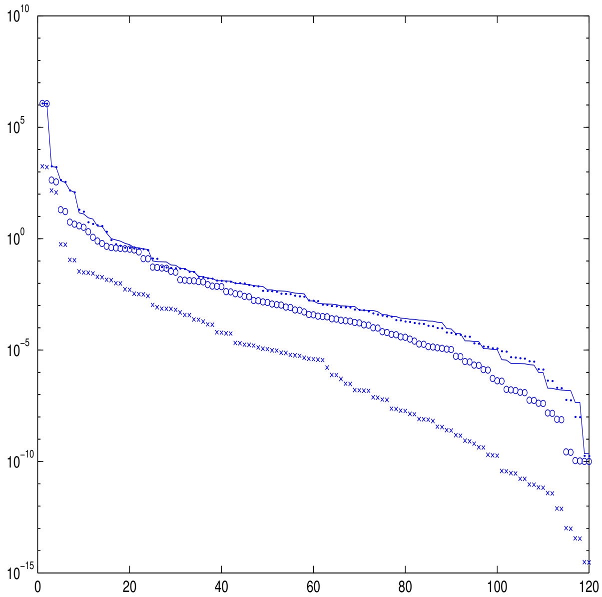

Figure 12: .. svd($\mathcal{G}_c$), o svd($\mathcal{G}_{c_1}$), x svd($\mathcal{G}_{c_2}$), ___ hsv

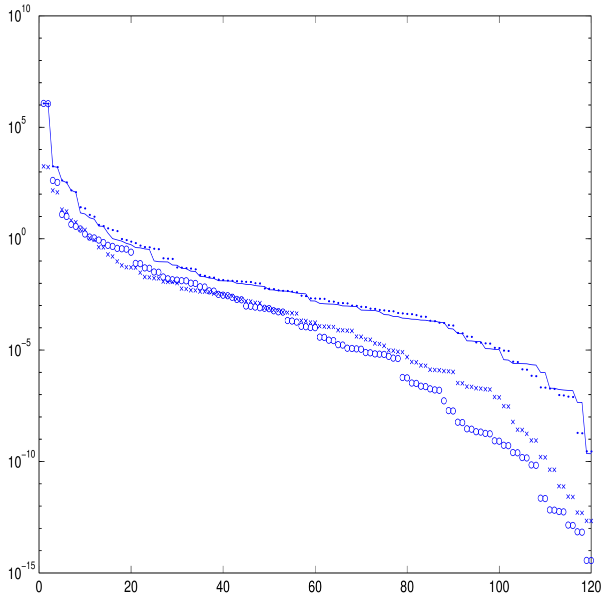

Figure 13: .. svd($\mathcal{G}_o$), o svd($\mathcal{G}_{o_1}$), x svd($\mathcal{G}_{o_2}$), ___ hsv

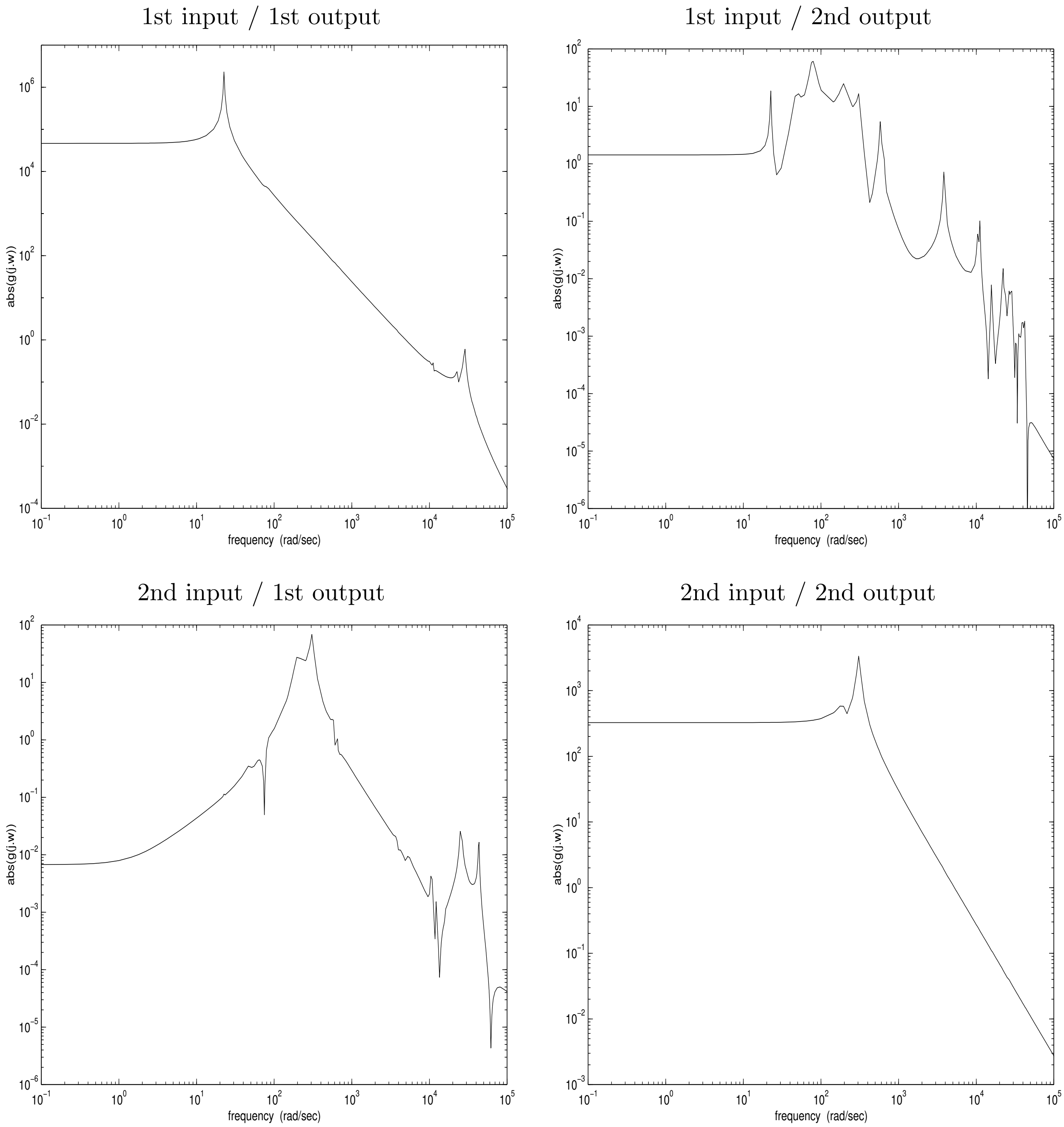

Figure 14: Frequency response of arm position controller.

2.4 PEEC model

This model arises from a partial element equivalent circuit (PEEC) model of a patch antenna structure [2],[6] and [7]. Containing 2100 capacitances, 172 inductances and 6990 mutual inductances, the circuit can be realized as a system of dimension 480. The couple (A, E) has an infinite eigenvalue $\lambda_\infty = -3.17\ .10^{44} + j2.27\ .10^{36}$, the other eigenvalues are shown in Figure.16.

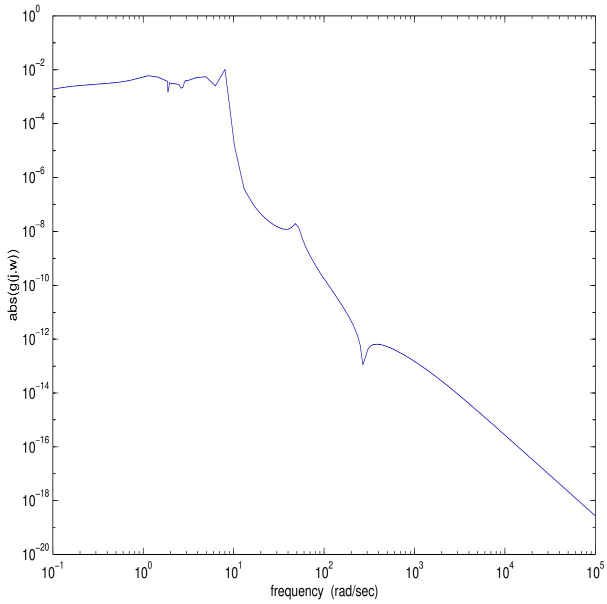

Figure 15: Frequency response.

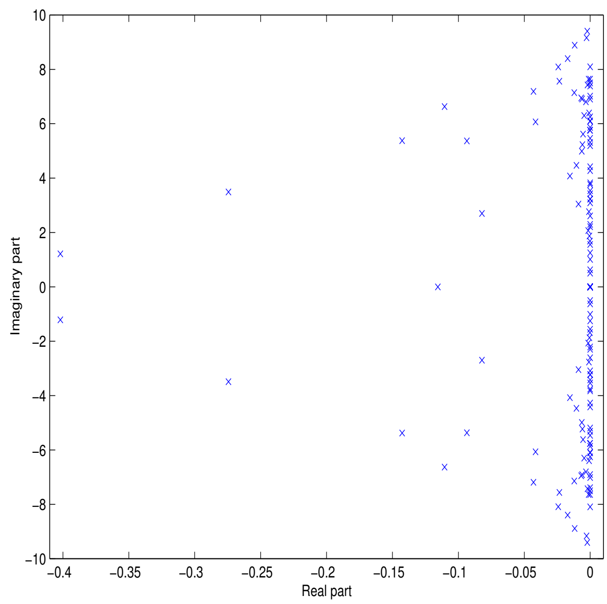

Figure 16: Generalized eigenvalues of (A, E).

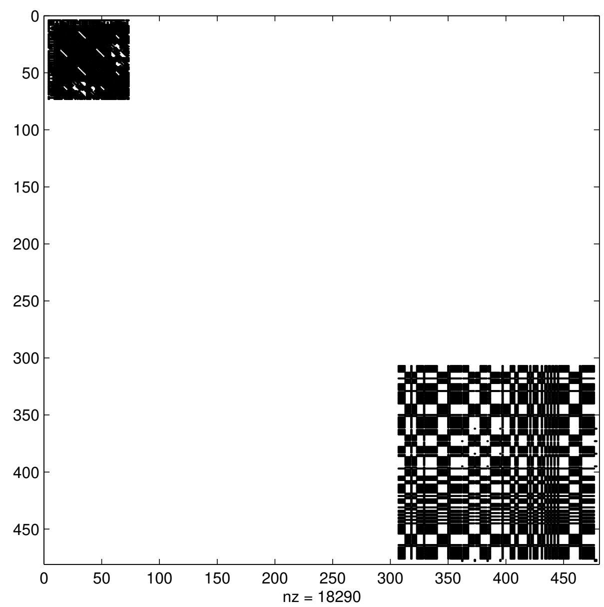

Figure 17: Sparsity E

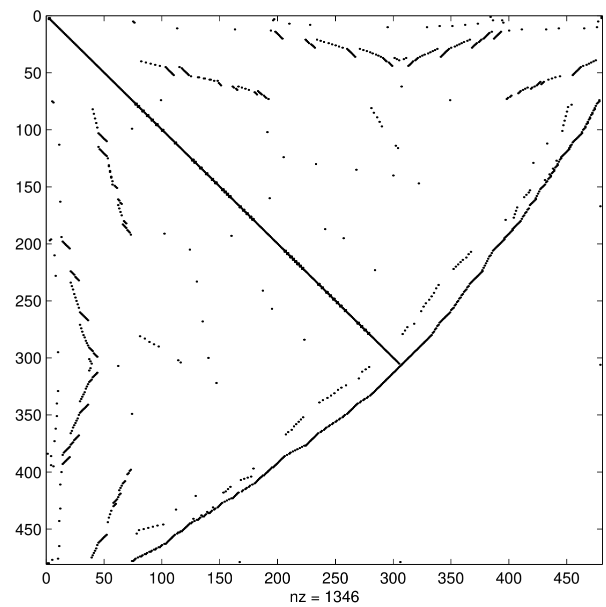

Figure 18: Sparsity A

2.5 FOM

This example is from [11]. It is a dynamical system of order 1006. The state-space matrices are given by

$$A = \begin{bmatrix} A_1 & & & \\ & A_2 & & \\ & & A_3 & \\ & & & A_4 \end{bmatrix} \; A_1 = \begin{bmatrix} -1 & 100 \\ -100 & -1 \end{bmatrix} \; A_2 = \begin{bmatrix} -1 & 200 \\ -200 & -1 \end{bmatrix} \; A_3 = \begin{bmatrix} -1 & 400 \\ -400 & -1 \end{bmatrix}$$

$$A_4 = diag(-1, \ldots, -1000), \quad B^T = C = [\underbrace{10 \;\ldots\; 10}_{6} \; \underbrace{1 \;\ldots\; 1}_{1000}]$$

the eigenvalues of A are: $\sigma(A) = \{-1, -2, \ldots, -1000, -1 \pm 100j, -1 \pm 200j, -1 \pm 400j, \}$

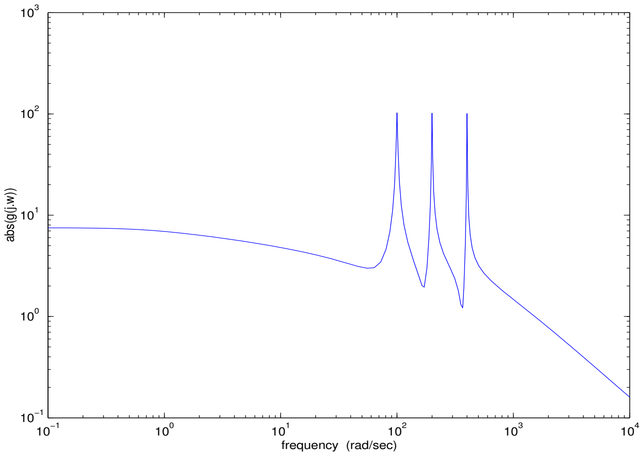

Figure 19: Frequency response.

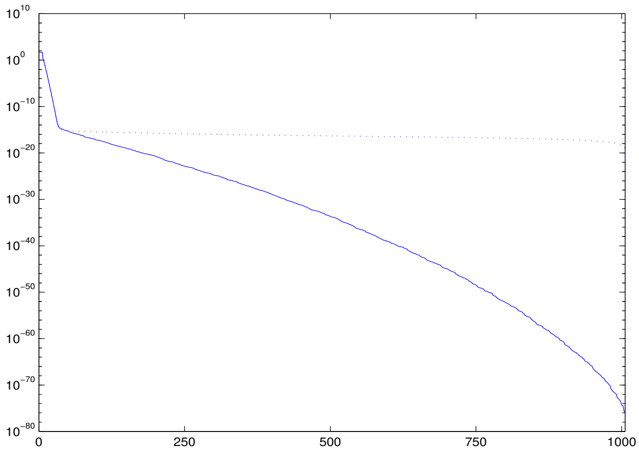

Figure 20: .. svd($\mathcal{G}_c$), o svd($\mathcal{G}_o$), ___ hsv

2.6 Random example

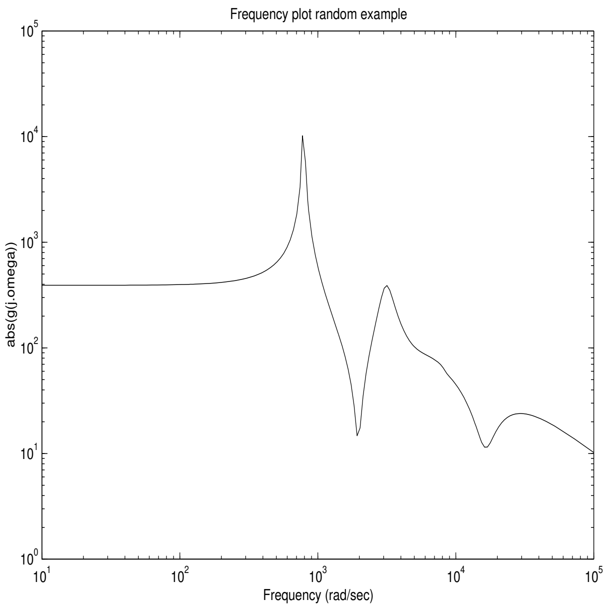

Figure 21: Frequency response.

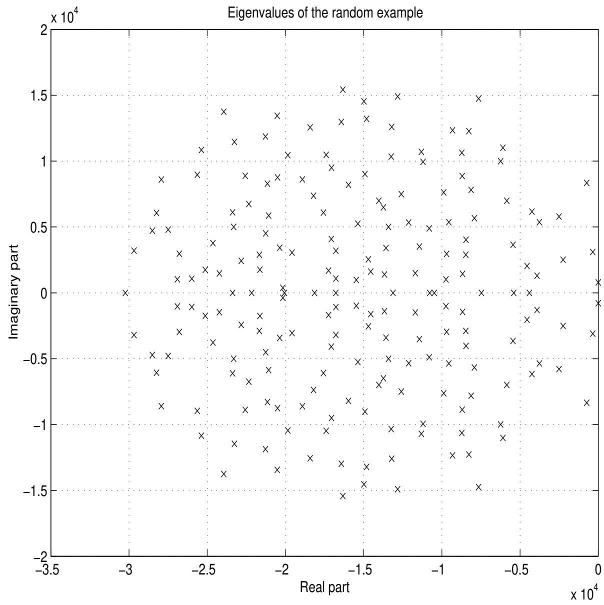

Figure 22: Eigenvalues of A

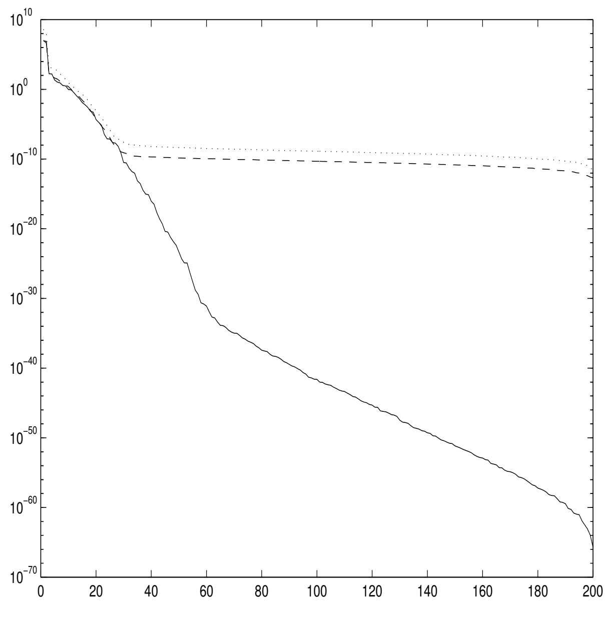

Figure 23: .. svd($\mathcal{G}_c$), _ _ svd($\mathcal{G}_o$), ___ hsv

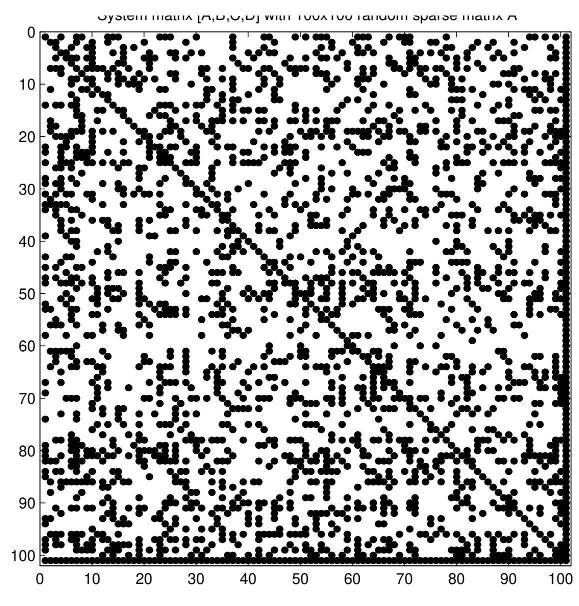

Figure 24: Sparsity of A.

2.7 PDE example

Consider the partial differential equation (PDE) [6],

$$\frac{\partial x}{\partial t} = \frac{\partial^2 x}{\partial z^2} + \frac{\partial^2 x}{\partial v^2} + 20\frac{\partial x}{\partial z} - 180x + f(v,z)u(t)$$

where x is a function of time (t), vertical position (v) and horizontal position (z). The boundaries of interest in this problem lie on a square with opposite corners at $(0,0)$ and $(1,1)$. The function $x(t,v,z)$ is zero on these boundaries. This PDE can be discretized with centered difference approximations on a grid of $n_v \times n_z$ points. The discretization grid, when $n_v = 3$ and $n_z = 5$, is shown in Figure.26. A state-space equation of dimension $N = n_v n_z$ results from the discretization. The sparsity pattern of the resulting A matrix, when $n_v = 7$ and $n_z = 12$, is shown in Figure.27. The input vector of the system corresponds to $f(v,z)$ and is composed of random elements. The output vector of the system is equated to the input vector for simplicity.

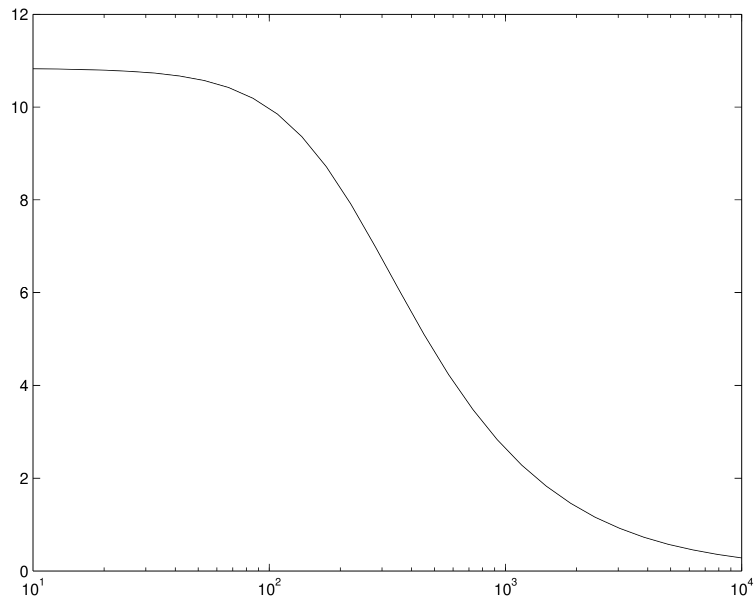

Figure 25: Frequency response.

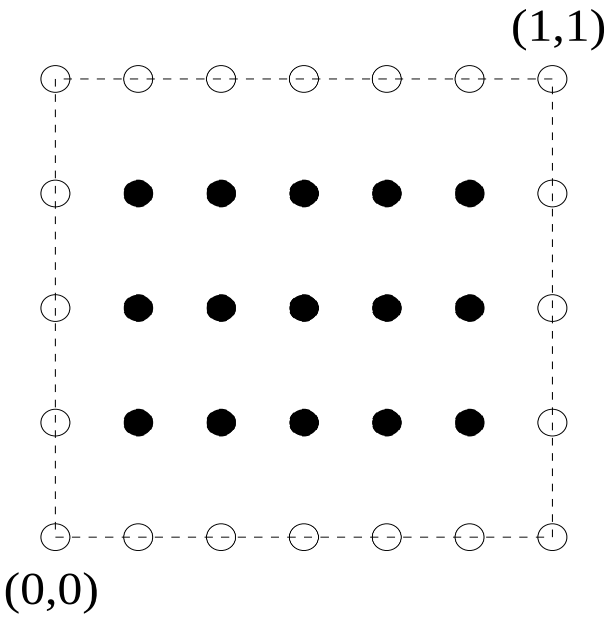

Figure 26: Discretization mesh, 3×5 case.

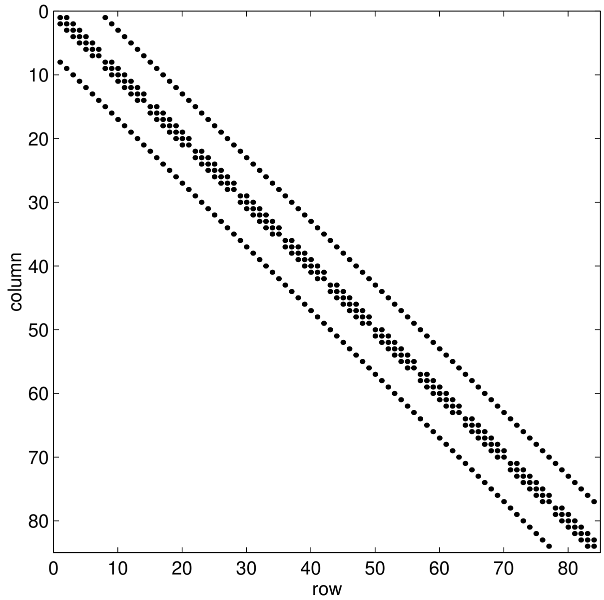

Figure 27: Sparsity of A.

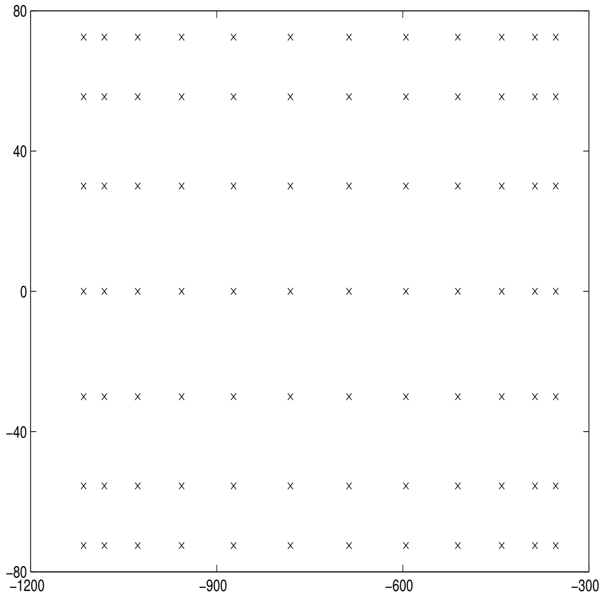

Figure 28: eigenvalue of A

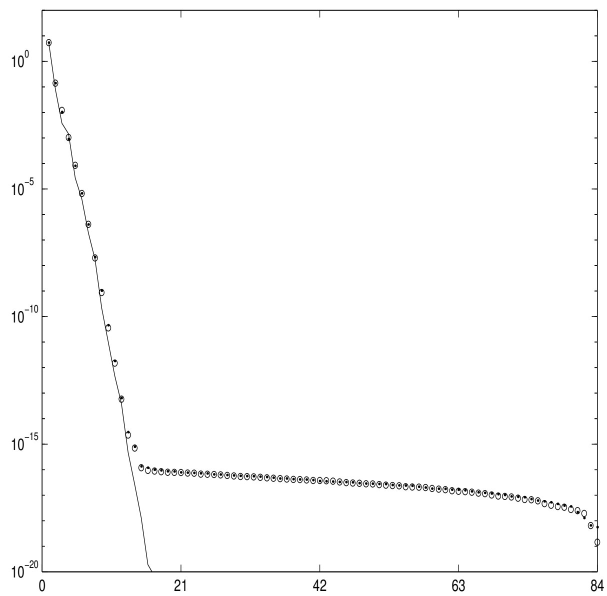

Figure 29: . svd($\mathcal{G}_c$), o svd($\mathcal{G}_o$), ___ hsv

2.8 Heat equation (cont. and discrete cases)

We consider the heat diffusion equation for the one-dimensional (1D) :

$$\begin{cases} \text{PDE} & \dfrac{\partial}{\partial t}T(x,t) = \alpha \dfrac{\partial^2}{\partial x^2}T(x,t) + u(x,t) & x \in (0,1); \quad t > 0 \\ \text{BCs} & T(0,t) = 0 = T(1,t) & t > 0 \\ \text{IC} & T(x,0) = 0 & x \in (0,1) \end{cases}$$

Where $T(x,t)$ represents the temperature field on a thin rod and $u(x,t) = u(t)\delta_{1/3}(x)$ is the heat source.
The solution is given by :

$$T(x,t) = x(x-1) + \sum_{i=0}^{\infty} \frac{8}{(2i+1)^3\pi^3} \sin((2i+1)\pi x) e^{-(2i+1)^2\pi^2\alpha t} + \Big(\int_0^t u(s)ds \Big) \delta_{1/3}(x)$$

The spatial domain is discretized into segments of length $h = \dfrac{1}{N+1}$.
Suppose for example that one wants to heat in a point of the rod located at 1/3 of the length and wants to record the temperature at 2/3 of the length.

We obtain the semi-discretized system :

$$\begin{cases} \dot{X}(t) = AX(t) + Bu(t) & ; \quad X(0) = 0 \\ Y(t) = CX(t) \end{cases}$$

where :

$$A = \frac{\alpha}{h^2} \begin{bmatrix} 2 & -1 & & & \\ -1 & 2 & -1 & & \\ & \ddots & \ddots & \ddots & \\ & & -1 & 2 & -1 \\ & & & -1 & 2 \end{bmatrix} \in \mathbb{R}^{N \times N}, \quad B = (\delta_{i,N/3})_i \in \mathbb{R}^N$$

$C = (\delta_{i,2N/3})_i^T \in \mathbb{R}^N$ and $X(t) \in \mathbb{R}^N$ is the solution evaluated at each x value in the discretization for t.
Now if we want to completely discretize the system, for example using Cranck-Nicholson we obtain :

$$\begin{cases} E_1X(k+1) = A_1X(k) + B_1u(k) & ; \quad X(0) = 0 \\ Y(k) = CX(k) \end{cases}$$

where $E_1 = I_N - \dfrac{\Delta t}{2}A, \quad A_1 = I_N + \dfrac{\Delta t}{2}A$ and $B_1 = \Delta t B$

Continuous case

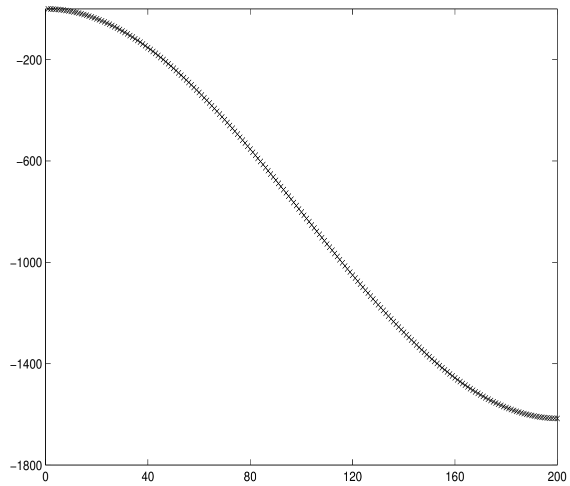

Figure 30: Eigenvalues of A

Discretized case

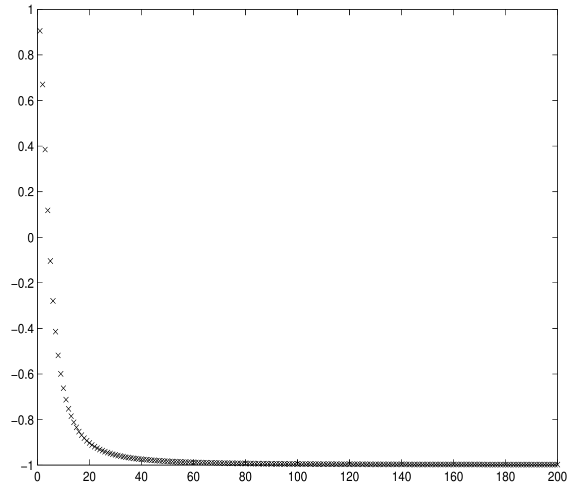

Figure 31: Generalized eigenvalues of $\lambda E - A$

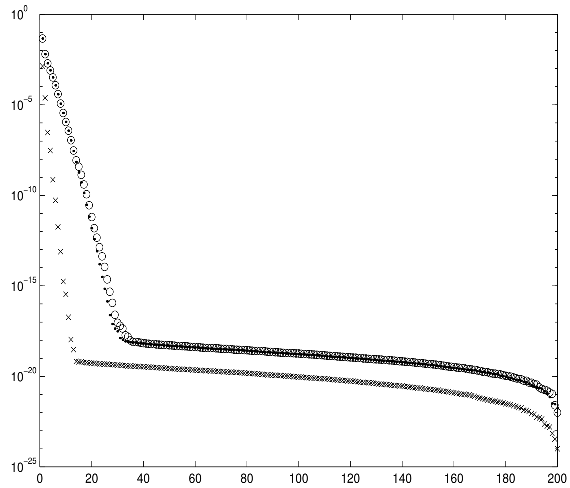

Figure 32: .. svd($\mathcal{G}_c$), o svd($\mathcal{G}_o$), x hsv

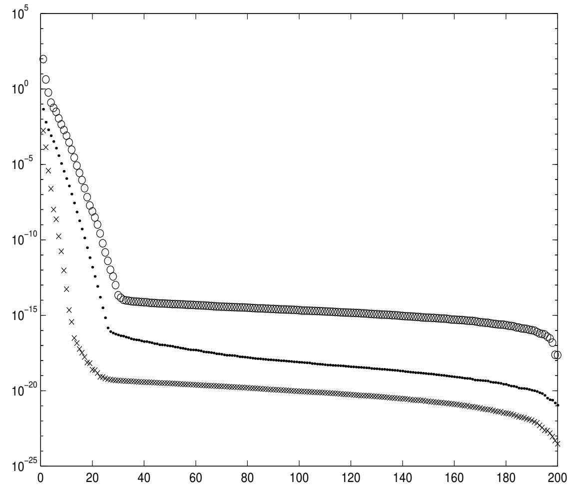

Figure 33: .. svd($\mathcal{G}_c$), o svd($\mathcal{G}_o$), x hsv

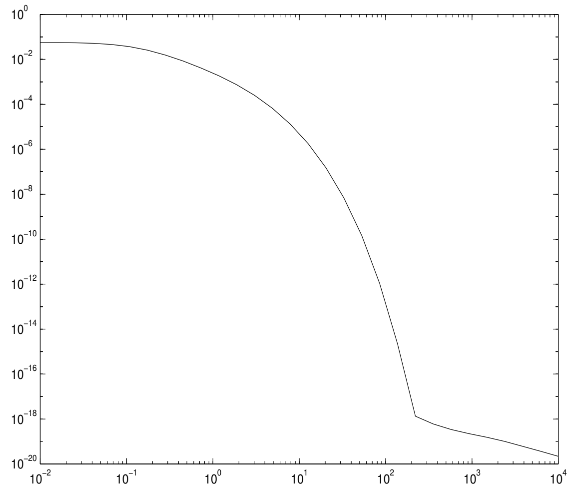

Figure 34: frequency response

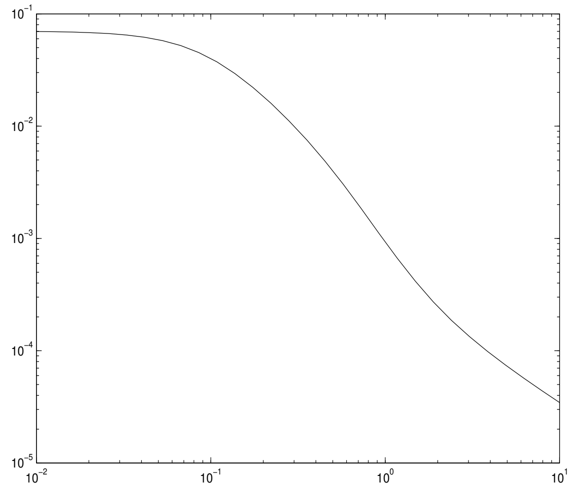

Figure 35: frequency response

2.9 Orr-Somerfeld example

The Orr-Sommerfeld operator for Couette flow (the mean velocity varies as $U = y$, y is the height) is in perturbation velocity variables [5]:

$$A = (-D^2)^{\frac{1}{2}} D^{-2} \Big(-ijkD^2 + \frac{1}{Re} D^4 \Big) (-D^2)^{-\frac{1}{2}}$$

where $D = \frac{d}{dy}$ and appropriate boundary conditions have been introduced (the perturbation velocities vanish at the walls) so that the inverse operators are defined. Re is the Reynolds number, and k is the x-wavenumber of the perturbation. This operator governs the evolution of 2-dimensional perturbations.
The matrix a 100×100 discretization for Reynolds number $Re = 800$ and $k = 1$ (this discretization gives accurate results for this Reynolds number).

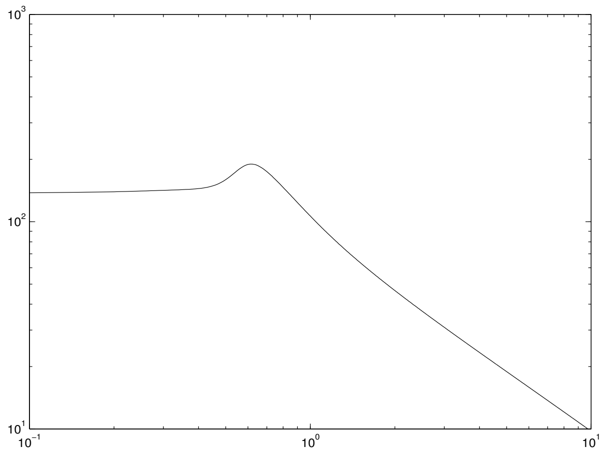

Figure 36: Frequency response.

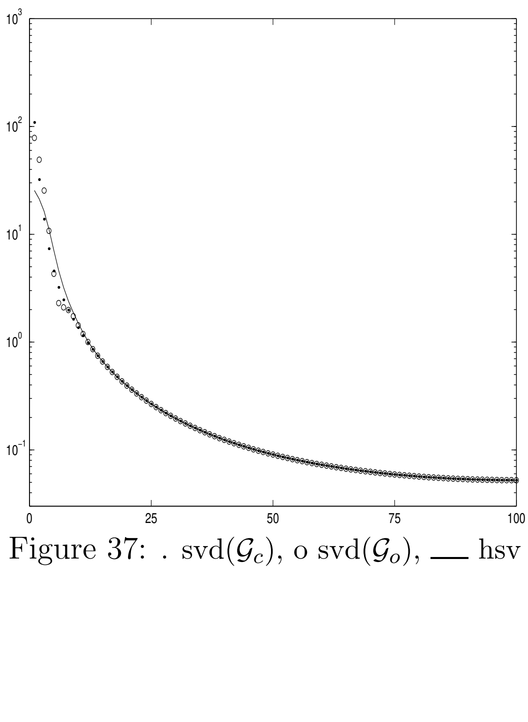

Figure 37: . svd($\mathcal{G}_c$), o svd($\mathcal{G}_o$), ___ hsv

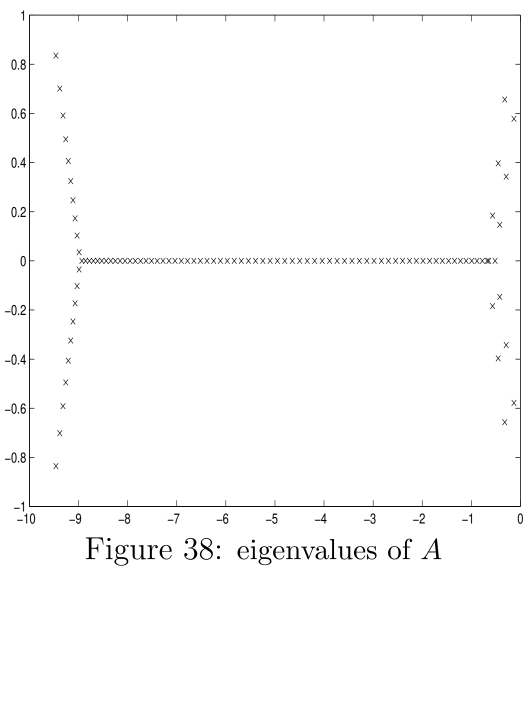

Figure 38: eigenvalues of A

2.10 MNA examples

To obtain the admittance matrix of a multiport, voltage sources are connected to the ports [10]. The multiport, along with these sources, constitutes the Modified Nodal Analysis (MNA) equations:

$$\begin{cases} E\dot{x}_n &= Ax_n + Bu_p \\ i_p &= Cx_n. \end{cases}$$

The i_p and u_p vectors denote the port currents and voltages, respectively, and

$$A = \begin{bmatrix} -N & -G \\ G^T & 0 \end{bmatrix}, \quad E = \begin{bmatrix} L & 0 \\ 0 & H \end{bmatrix} \quad x_n = \begin{bmatrix} v \\ i \end{bmatrix}$$

where v and i are the MNA variables corresponding to the node voltages, inductor and voltage source currents, respectively. The $n \times n$ matrices $-A$ and E represent the conductance and susceptance matrices, while $-N$, L and H are the matrices containing the stamps for resistors, capacitors and inductors, respectively. G consists of 1, -1 and 0, which represent the current variables in KCL equations. Provided that the original N-port is composed of passive linear elements only, L, H and $-N$ are symmetric nonnegative definite matrices. This implies that E is also symmetric and nonnegative definite. Since this is an N-port formulation, whereby the only sources are the voltage sources at the N port nodes, $B = C^T$. The E matrices all have several singular modes.

We have five sparse examples:

name of file	dimension
MNA_1	578
MNA_2	9223
MNA_3	4863
MNA_4	980
MNA_5	10913

We show above only the characteristics of the fourth example.

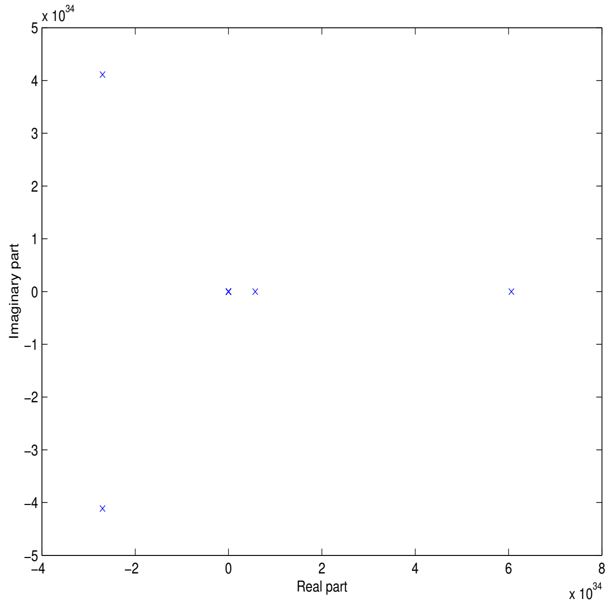

Figure 39: generalized eigenvalue of (E, A)

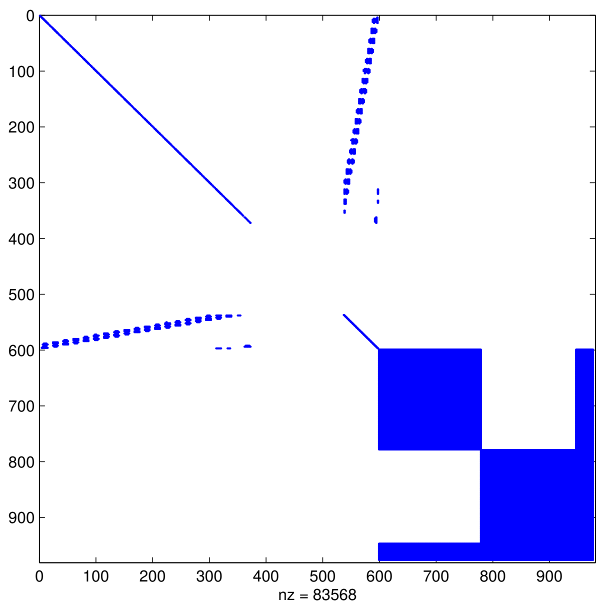

Figure 40: sparsity E

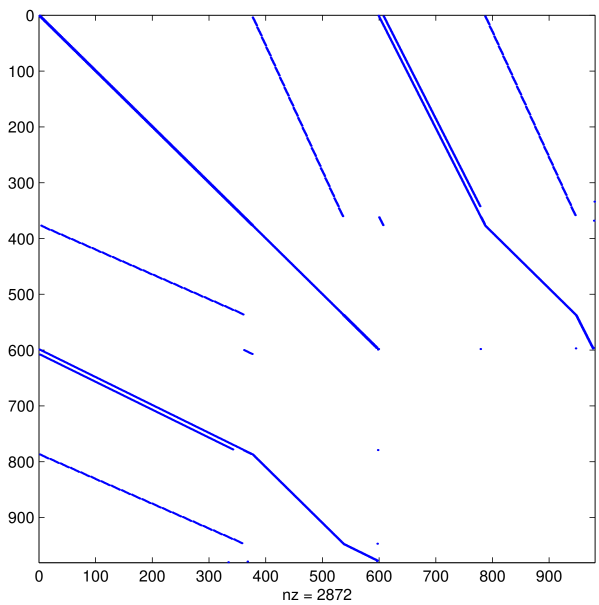

Figure 41: sparsity A

2.11 International space station

It is a structural model of component 1r (Russian service module) of the International Space Station (ISS) [1].

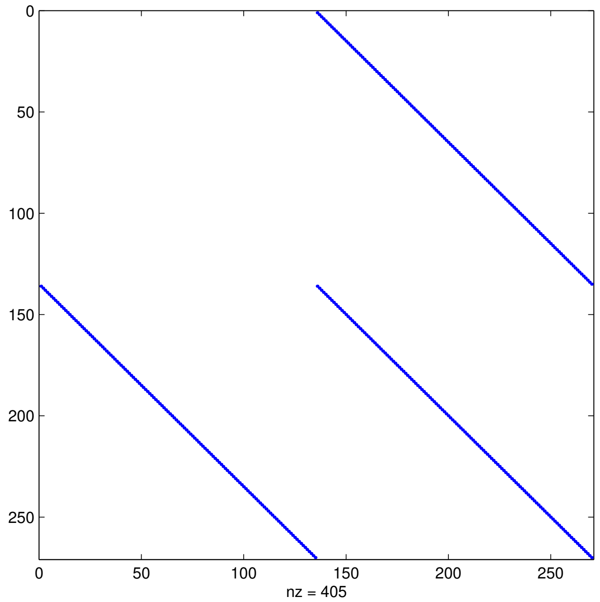

Figure 42: Sparsity of A.

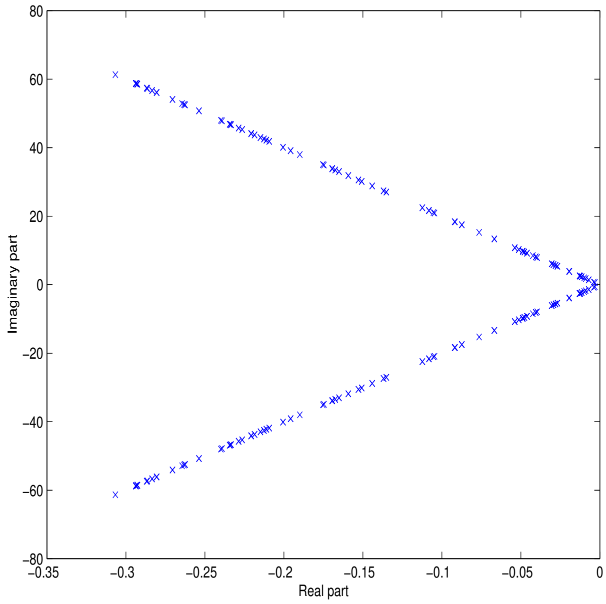

Figure 43: Eigenvalues of A.

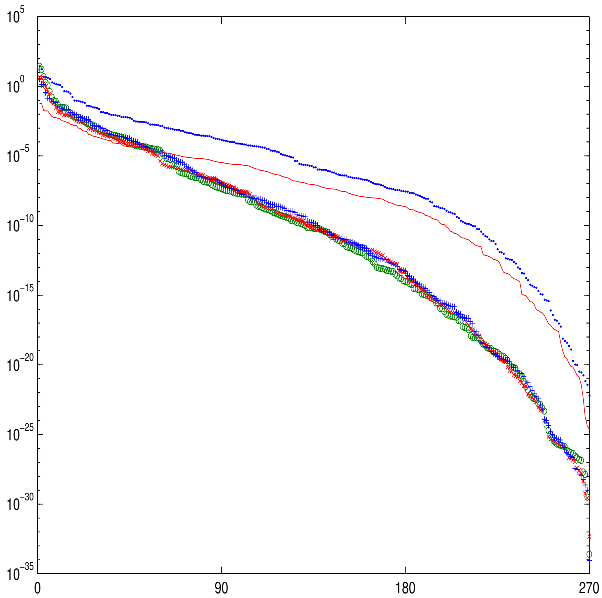

Figure 44: .. svd($\mathcal{G}_c$), o svd($\mathcal{G}_{c_1}$), x svd($\mathcal{G}_{c_2}$), + svd($\mathcal{G}_{c_3}$), ___ hsv

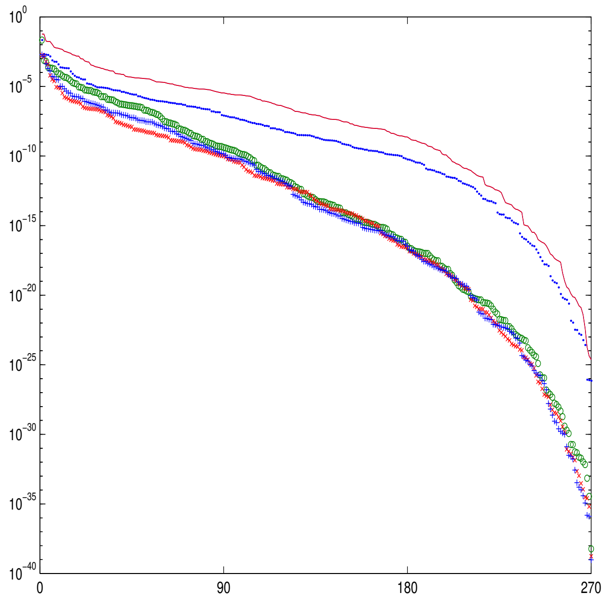

Figure 45: .. svd($\mathcal{G}_o$), o svd($\mathcal{G}_{o_1}$), x svd($\mathcal{G}_{o_2}$), + svd($\mathcal{G}_{o_3}$), ___ hsv

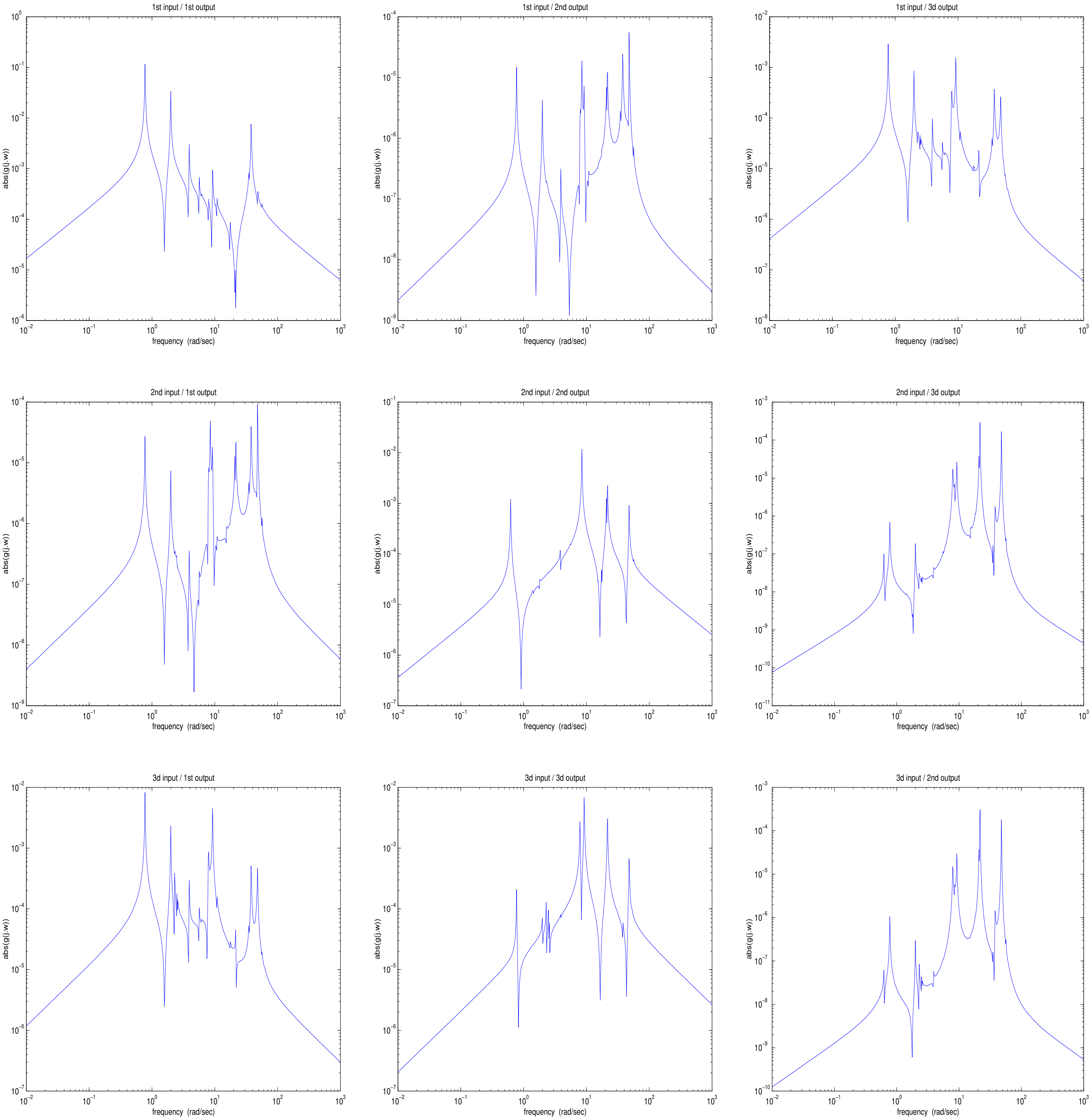

Figure 46: Frequency response of the ISS model.

2.12 Building model

It is a model of a building (the Los Angeles University Hospital) with 8 floors each having 3 degrees of freedom, namely displacements in x and y directions, and rotation [1]. Hence we have 24 variables with a polynomial system:

$$M\ddot{q}(t) + C\dot{q}(t) + Kq(t) = vu(t)$$

where $u(t)$ is the input. This system can be put into a traditional state space form of order 48 by defining $x = \begin{bmatrix} q \\ \dot{q} \end{bmatrix}$. We are mostly interested in the motion in the first coordinate $q_1(t)$. Hence, we choose $v = \begin{bmatrix} 1 & 0 & \dots & 0 \end{bmatrix}^T$ and the output $y(t) = \dot{q}_1(t) = x_{25}(t)$.

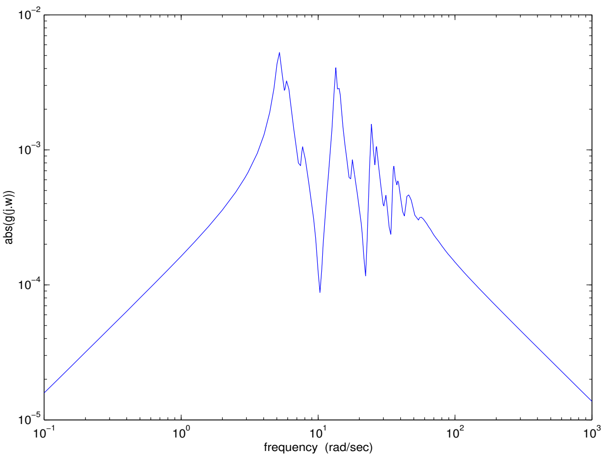

Figure 47: Frequency response.

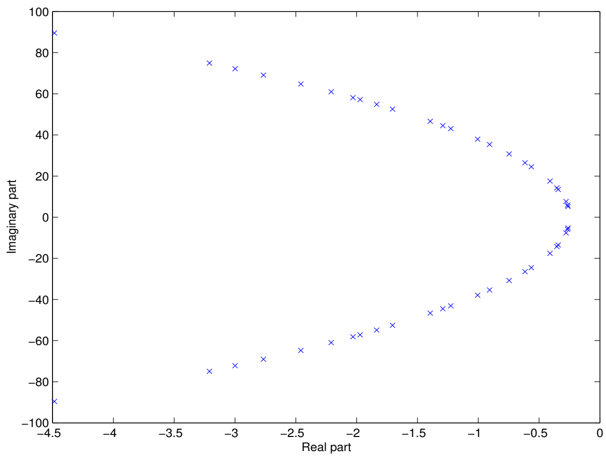

Figure 48: Eigenvalues of A

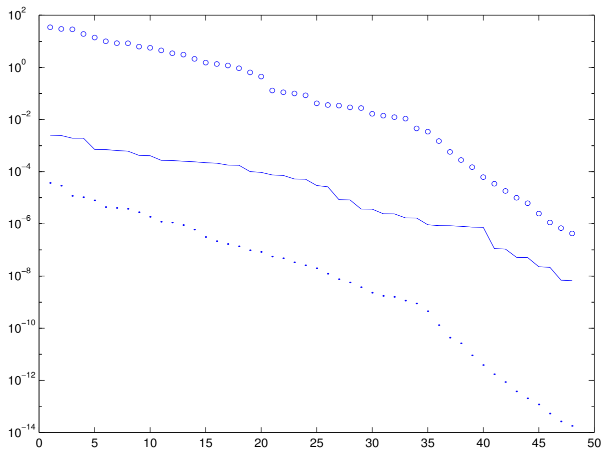

Figure 49: .. svd($\mathcal{G}_c$), o svd($\mathcal{G}_o$), ___ hsv

2.13 Clamped beam model

The clamped beam model has 348 states, it is obtained by spatial discretization of an appropriate partial differential equation [1]. The input represents the force applied to the structure at the free end, and the output is the resulting displacement.

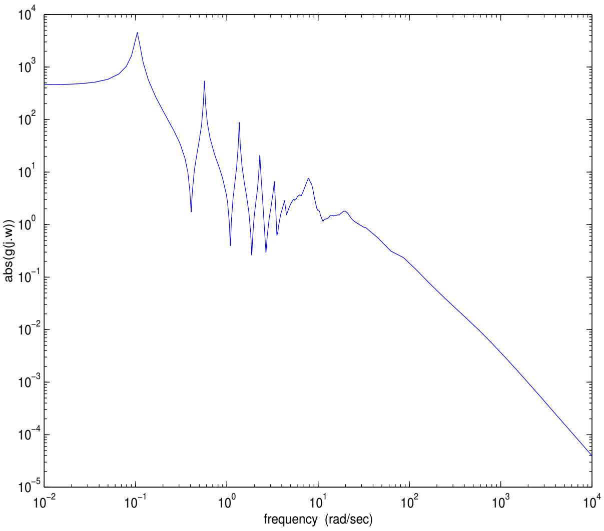

Figure 50: Frequency response.

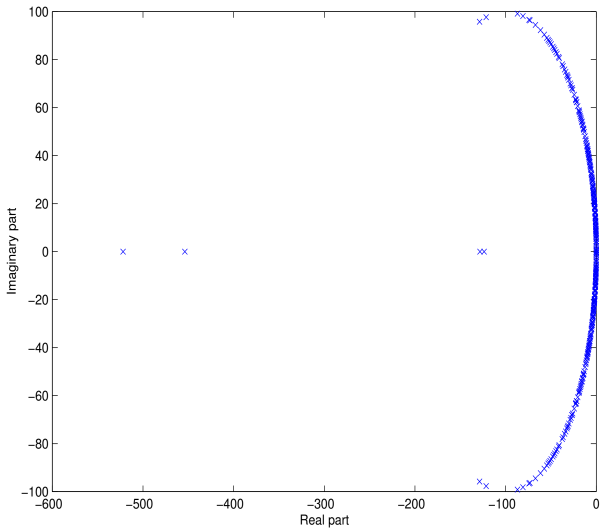

Figure 51: Eigenvalues of A

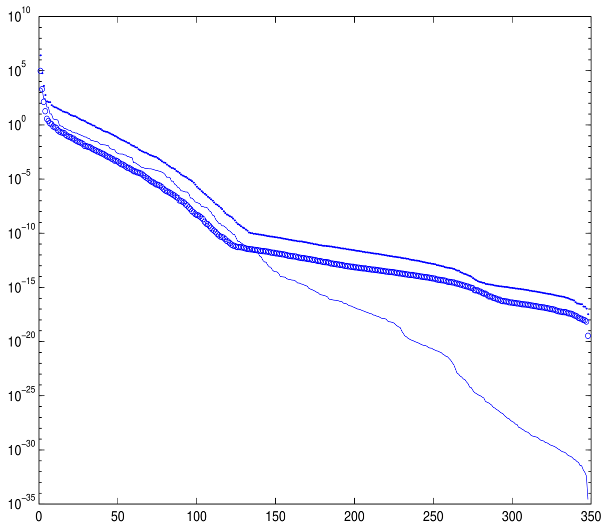

Figure 52: .. svd($\mathcal{G}_c$), o svd($\mathcal{G}_o$), ___ hsv

3 Acknowledgement

We would like to thank T. Antoulas, S. Gugercin, B. Farrell, P. Ioannou and J. R. Li for contributing some of the examples.

References

[1] A. C. Antoulas, D. C. Sorenson and S. Gugercin, " A Survey of Model Reduction Methods for Large-Scale Systems", *Contemporary Mathematics, 280, pp.193–219, 2001.*

[2] E. Chiprout and M. S. Nakhla, "Asymptotic Waveform Evaluation and Moment Matching for Interconnect Analysis", *Boston, MA : Kluwer Academic Publishers, 1994.*

[3] Y. Chahlaoui, D. Lemonnier, K. Meerbergen, A. Vandendorpe and P. Van Dooren, "Model Reduction of Second Order Systems", *accepted to MTNS2002.*

[4] W. Draijer, M. Steinbuch and O. H. Bosgra, "Adaptive Control of the Radial Servo System of a Compact Disc Player", *IFAC Automatica, vol 28, no.3, pp.455–462, 1992.*

[5] B. F. Farrell and P. J.Ioannou, "Accurate Low Dimensional Approximation of the Linear Dynamics of Fluid Flow", *American Meteorological Society, pp. 2771–2789, 2001.*

[6] E. J. Grimme, "Krylov Projection Methods for Model Reduction", *Ph. D in the Graduate College of the University of Illinois at Urbana-Champaign, 1997*

[7] H. Heeb, A. E. Ruehli, J. E. Bracken, and R. A. Rohrer, "Three Dimensional Circuit Oriented Electromagnetic Modeling for VLSI Interconnects", *Proc. IEEE Int. Conf. Computer Design, Cambridge, MA, pp. 218–221, 1992.*

[8] J. R. Li and J. White, "Efficient Model Reduction of Interconnect via Approximate System Gramians", *Proceedings of the IEEE/ACM International Conference on Computer-Aided Design, pp.380–383, 1999.*

[9] N. Marques, M. Kamon, J. White and L. M. Silveira, "A Mixed Nodal-Mesh Formulation for Efficient Extraction and Passive Reduced-Order Modeling of 3D Interconnects", *Proceedings of the 35th IEEE/ACM Design Automation Conference,San Fransisco, CA, pp.297–302, 1998.*

[10] A. Odabasioglu, M. Celik and L. T. Pileggi, "PRIMA: Passive Reduced-order Interconnect Macromodeling Algorithm", *IEEE Transactions on Computer-Aided Design of Integrated Circuits and Systems, vol.17, no.8, pp.645–654, 1998.*

[11] T. Penzl, "Algorithms for Model Reduction of Large Dynamical Systems", *TR SFB393/99-40, Sonderforschungsbereich 393 Numerische Simulation auf massiv parallel Rechern, TU Chemnitz, 09107, FRG, 1999.*

[12] Y. Saad, "Projection and Deflation Methods for Partial Pole Assignment in Linear State Feedback", *IEEE Trans. Autom. Control, vol.33, pp.290–297, 1988.*

[13] P. M. R. Wortelboer, M. Steinbuch and O. H. Bosgra, "Closed-Loop Balanced Reduction with Application to a Compact Disc Mechanism", *Selected Topics in Identification, Modeling and Control, vol.9, Delft University Press, December 1996.*